Pergamon

NanoStructured Materials, Vol. 5, No. 3, pp. 257-268, 1995

0965-9773/95 $9.50 + .00

0965-9773(95)00246-4

THEORETICAL INVESTIGATION OF THE THERMODYNAMIC STABILITY OF NANO-SCALE SYSTEMS—I: PERIODIC LAYER-STRUCTURES

R.Kikuchi[1] and L.-Q. Chen[2]

[1] Department of Materials Science and Engineering, University of California at Los Angeles, CA 90024-1595
[2] Department of Materials Science and Engineering, Pennsylvania State University, University Park, PA 16802

(Accepted February 1995)

Abstract—*The thermodynamic stability of periodic layer-structures is analyzed theoretically using equilibrium statistical mechanics. While the system itself is not in complete thermodynamic equilibrium, it can be stable under appropriate constraint conditions and its stability can be determined by minimizing the free energy in the constrained state. A model binary FCC system with a miscibility gap is treated using the pair approximation of the Cluster Variation Method. A symmetric system with an overall average composition 50 atom % A and 50 atom % B is considered. It is shown that the equilibrium compositions of two phases in a periodic layer-structure depend strongly on the periodicity when the composition wavelength is decreased down to a few nanometers. The result reveals that the mutual solubilities of two materials increase significantly as the layer-thickness decreases. In an extreme case, they may become totally miscible.*

INTRODUCTION

Usual treatment of thermodynamic stability and phase equilibria of a system considers only the bulk free energies of various phases involved. At constant temperature and pressure, the equilibrium compositions or mutual solubilities among the phases are determined by the condition that the chemical potential of each component is uniform throughout the system. The surface and interphase interfacial energy contributions to the total free energy are completely ignored. For systems of macro-scale size (>> the correlation length), such a treatment is totally appropriate and adequate. However, as the size of the system decreases, for example, down to the nanoscale, as in nano-crystalline particles and nanoscale or atomic-scale thin films, the usual thermodynamic treatment becomes problematic. There is a high percentage of atoms located at or affected by the interfaces or the interfacial regions. The contribution from the surface and interfacial energy to the total free energy may become comparable to the bulk free energy and hence can not be ignored. As a result, the phase stability and phase diagram of a nanoscale system could be dramatically different from the corresponding macroscopic ones. A clear indication of the importance of the surface and interfacial energy contribution is the shift of phase transition temperatures in some

nanoscale systems (1). For example, the melting temperature of nanoscale metallic particles was found to decrease sharply as the size decreases (2). The ferroelectric transition temperature of ferroic materials decreases as the grain size or the thickness of a thin film is reduced (3). In the extreme case, the ferroelectric phase transition may totally disappear. Such a shift of phase boundary or phase transition temperature due to the small size is called the "size effect" (1). It has drawn much attention recently due to the technological desire to fabricate increasingly small electronic devices.

Modern experimental techniques such as Molecular Beam Epitaxy (MBE) are now able to synthesize atomic- or nanoscale thin films as well as multi-layer structures made up of alternating layers of different materials. For multilayer structures, the stability against interdiffusion and coarsening becomes a critical issue at finite temperatures. It is qualitatively clear that the stability of such layers against interdiffusion is determined by both thermodynamics and kinetics. Similar to the phase boundary shift due to the particle size, the phase stability of such atomic scale and nanoscale layer-structure should strongly depend on the layer-thickness. In particular the mutual solubilities among the phases should be strong functions of layer-thickness in those nanoscale layer structures. However, the rate of interdiffusion to reach the thermodynamic equilibrium is determined by the interdiffusion kinetics. We will consider only the thermodynamic stability of nanoscale layer-structures in this paper. The highly nonlinear kinetics of interdiffusion and coarsening of the layer-structure will be discussed in another publication.

We consider a model system which is a periodic layer structure made up of α and β phases. We assume α and β phases have the same zinc blende structure with one of the FCC sublattices fully occupied by C atoms. The other FCC sublattice is occupied by either A atoms in the pure α phase or B atoms in the pure β phase. We assume that at low temperatures α and β phases have very limited mutual solubility and at very high temperatures they are mutually soluble, *i.e.*, the phase diagram of the system ($A_xB_{1-x}C$) exhibits a miscibility gap. The main objective of this paper is to determine the dependence of phase diagram (temperature-composition diagram) on the layer-thickness. If the as-deposited layers are pure α and β phases, the mutual solubility determined from the miscibility gap is an indication of the thermodynamic stability of layer-structure against interdiffusion. It may be qualitatively expected, at a given temperature, that the mutual solubilities of the two phases should increase as the layer-thickness decreases.

To calculate the phase diagram for such nanoscale layer-structures, we can employ the equilibrium statistical mechanics method, namely, the pair approximation of the Cluster Variation Method (CVM) (4), although the structure is only metastable. CVM has been extensively used in the equilibrium phase diagram calculations for alloy systems including multicomponent semiconductor alloys. However, as far as the authors are aware of, this is the first CVM work which includes the interfacial energy contribution in the phase diagram calculation. As we discussed above, the interfacial energy contribution becomes crucial for atomic- and nanoscale systems. We expect the results will also shed light on other related problems, such as the solubility of impurities as a function of the grain size in nanocrystalline materials.

CVM FORMULATION OF THE LAYERED STRUCTURE

In the CVM method, we first have to specify state variables which describe the thermodynamic state of a system and then the equilibrium state of the given system is obtained by minimizing the total free energy with respect to the state variables. Since the system that we

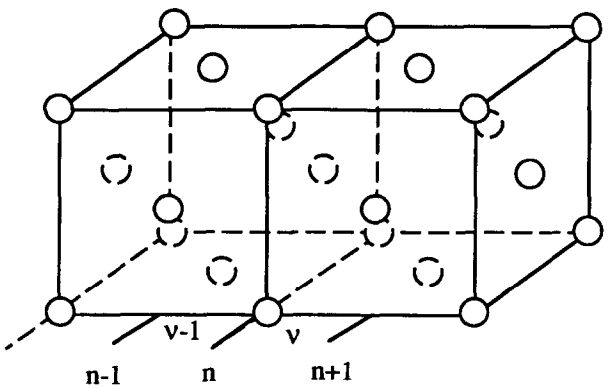

Figure 1. Designation of the lattice plane, n, and the bond, ν, in the (100) layer-structure of the FCC lattice.

consider is a pseudobinary alloy, AC-BC, with AC and BC having the same crystal structure, we only need to specify state variables related to atoms A and B. We employ the pair approximation for the thermodynamic description in which the state variables are the point variables, $x(i)$, and the pair variables $y(ij)$, where i,j = A or B. It is reminded that the classical Bragg-Williams model considers only the point variables, and also that the tetrahedron cluster is not needed to obtain reasonably accurate results since the system exhibits phase separation instead of ordering although the lattice is FCC. It is assumed that the layer-structure is along the (100) direction of the FCC sublattice. Therefore, the point and pair variables vary along this direction. To distinguish the atomic pairs within a (100) plane and the atomic pairs connecting two neighboring (100) planes, we number the lattice planes and bonds with n and ν as illustrated in Figure 1. Therefore, there will be three kinds of state variables, $x_n(i)$, $y_n(ij)$ and $y_\nu(ij)$. $x_n(i)$ is the probability of finding an i atom at a lattice point at n, $y_n(ij)$ is the probability of finding an ij pair on a bond on an nth plane, and $y_\nu(ij)$ is the probability of finding i on an n point and j on an adjacent n+1 point.

The point and pair variables are subject to the following normalization and reduction conditions:

$$\sum_i x_n(i) = 1$$

$$\sum_i \sum_j y_n(ij) = 1; \qquad \sum_i \sum_j y_\nu(ij) = 1$$

$$\sum_j y_n(ij) = x_n(i); \qquad \sum_j y_\nu(ij) = x_n(i); \qquad \sum_j y_{\nu-1}(ji) = x_n(i) \qquad [1]$$

To calculate the phase diagram, we use the grand potential, Ω, as the thermodynamic potential function to be minimized. In the pair approximation, the total grand potential for the layer-structure is given by

$$\Omega \equiv \sum_\nu \Omega_\nu + \sum_n \Omega_n \qquad [2]$$

where the first and second terms are the contributions from the ν and n bonds, respectively. Instead of directly working with the grand potential, we define a dimensionless potential

$$\Psi \equiv \frac{\beta\Omega}{N} = \sum_{\nu} \frac{\beta\Omega_{\nu}}{N} + \sum_{n} \frac{\beta\Omega_{n}}{N} = \sum_{\nu} \Psi_{\nu} + \sum_{n} \Psi_{n} \qquad [3]$$

where β is equal to $1/k_B T$, N is the total number of lattice points on the plane, n.

Our purpose is to minimize Ψ with respect to the pair variables, $y_{\nu}(ij)$ and $y_n(ij)$, to obtain the equilibrium state for the layer-structure. From the normalization conditions for pair variables, they are subject to the following two constraints at every n and for i:

$$\sum_{j} y_{\nu-1}(ji) = \sum_{j} y_{\nu}(ij) \qquad [4]$$

and

$$\sum_{j} y_{\nu-1}(ji) + \sum_{j} y_{\nu}(ij) = 2\sum_{j} y_n(ij) \qquad [5]$$

The potential function together with the constraints to be minimized is then

$$\begin{aligned}\Psi_{\nu} \equiv \frac{\beta\Omega_{\nu}}{N} &= 4\beta\sum_{ij}\varepsilon(ij)y_{\nu}(ij) - \frac{11}{3}\left\{\sum_{i}\left[L\left(x_n^{[1]}(i)\right)+1\right]\right\} + \sum_{j}\left[L\left(x_{n+1}^{[2]}(j)\right)+1\right] \\ &+ 4\sum_{ij}\left[L(y_{\nu}(ij))+1\right] - \frac{1}{3}\beta\sum_{ij}\left[\mu(i)+\mu(j)\right]y_{\nu}(ij) \\ &+ 4\beta\lambda_{\nu}\left[1-\sum_{ij}y_{\nu}(ij)\right] + 4\sum_{ij}\left[\kappa_n(i)+\kappa_{n+1}(j)\right]y_{\nu}(ij) - 4\sum_{ij}\left[\gamma_n(i)-\gamma_{n+1}(j)\right]y_{\nu}(ij)\end{aligned}$$

$$\begin{aligned}\Psi_n \equiv \frac{\beta\Omega_n}{N} &= 2\beta\sum_{ij}\varepsilon(ij)y_n(ij) - \frac{11}{6}\left\{\sum_{i}\left[L\left(x_n^{[3]}(i)\right)+1\right]\right\} + \sum_{j}\left[L\left(x_n^{[3]}(j)\right)+1\right] \\ &+ 2\sum_{ij}\left[L(y_n(ij))+1\right] - \frac{1}{6}\beta\sum_{ij}\left[\mu(i)+\mu(j)\right]y_n(ij) \\ &+ 2\beta\lambda_n\left[1-\sum_{ij}y_n(ij)\right] - 4\sum_{ij}\left[\kappa_n(i)+\kappa_n(j)\right]y_n(ij)\end{aligned} \qquad [6]$$

where the Lagrange multipliers, $4\gamma_n(i)$ and $4\kappa_n(i)$, are for the constraints [4] and [5], respectively, $2\lambda_{\nu}$ and $2\lambda_n$ for the normalization conditions in [1], $L(x) \equiv x\ln(x) - x$, $\varepsilon(ij)$ is the energy for the ij pair, and $x_n^{[1]}(i)$, $x_{n+1}^{[2]}(j)$ and $x_n^{[3]}(j)$ are given by the reduction relations

$$x_n^{[1]}(i) = \sum_{j} y_{\nu}(ij); \qquad x_{n+1}^{[2]}(j) = \sum_{i} y_{\nu}(ij); \qquad x_n^{[3]}(i) = \sum_{j} y_n(ij) = \sum_{j} y_n(ji) \qquad [7]$$

The Lagrange multipliers, λ_ν and λ_n, have special meaning: we can show that when Ψ is minimized, it is simplified as

$$\Psi \equiv \frac{\beta\Omega}{N} = \sum_{\nu} 4\beta\lambda_\nu + \sum_{n} 2\beta\lambda_n \qquad [8]$$

Minimizing Ψ' s with respect to $y_\nu(ij)$ and $y_n(ij)$, we obtain the following basic equations,

$$y_\nu(ij) = \exp\left\{\beta\lambda_\nu - \beta\varepsilon(ij) + \frac{\beta}{12}[\mu(i)+\mu(j)] - [\kappa_n(i)+\kappa_{n+1}(j)] + [\gamma_n(i)-\gamma_{n+1}(j)]\right\}$$
$$[x_n(i)x_{n+1}(j)]^{\frac{11}{12}}$$

$$y_n(ij) = \exp\left\{\beta\lambda_n - \beta\varepsilon(ij) + \frac{\beta}{12}[\mu(i)+\mu(j)] + 2[\kappa_n(i)+\kappa_n(j)]\right\}[x_n(i)x_n(j)]^{\frac{11}{12}} \qquad [9]$$

When the system is homogeneous, $\kappa_n(i) = \lambda_n(i) = 0$ and these two expressions reduce to the known equation for $y(ij)$ in the FCC. The equations in [9] are nonlinear equations which have to be solved numerically.

NIM SOLUTION OF THE BASIC EQUATIONS

Because of the special nature of the layered structure we found that it is easier to solve the basic equations using the Natural Iteration Method (NIM) (5) than the Newton-Raphson method. The procedure of solving the basic equations are as follows.

(i) Specify the Thermodynamic Conditions by Assigning Values for the Temperature, thus β, and the Chemical Potential, μ.

In a binary system without considering vacancies, we can set $\mu(A)+\mu(B)=0$, so that we may define μ as

$$\mu(A) = -\mu; \qquad \mu(B) = \mu \qquad [10]$$

In the Ising model assignment of energy parameters, we can choose $\mu = 0$ because this is the value for the coexistence of the two phases.

(ii) Assign Initial Values of $x_n(i)$, $y_n(ij)$ and $y_\nu(ij)$.

The NIM treatment of the equations starts with the initial guess values of $x_n(i), y_n(ij)$ and $y_\nu(ij)$. For the binary system without vacancies, we need $x_n(A)$ and $x_n(B)$ for all n which determine the layer-thickness. As an advantage of the NIM, we do not need to start with $x_n(A)$ which are close to the final solution. As a matter of fact, since we are only interested in the

final state of the layer structure instead of the interdiffusion kinetics, we may choose any initial condition which satisfies the required symmetry and layer-thickness. For example

$$\begin{aligned} x_n(1) &= 0.8 \quad \text{for } 1 \le n \le n_1 \\ x_n(1) &= 0.2 \quad \text{for } n_1 + 1 \le n \le 2n_1 \end{aligned} \tag{11a}$$

can lead to a symmetric layer-structure solution in which $x_n(1) > 0.5$ in $1 \le n \le n_1$, and $x_n(1) < 0.5$ in $n_1 + 1 \le n \le 2n_1$. The simple choice of the initial values of $y_n(ij)$ and $y_\nu(ij)$ is to make them uncorrelated, *i.e.*,

$$y_n(ij) = x_n(i)x_n(j); \text{ and } y_\nu(ij) = x_n(i)x_{n+1}(j) \tag{11b}$$

(iii) Use Minor Iterations to Solve the Lagrange Multiplier κ_n

Starting with the initial values of $y_n(ij)$ and $y_\nu(ij)$, we first solve $\kappa_n(i)$ in the minor iterations to satisfy [5]. When equations in [9] are used in [5], we write

$$\exp[-\kappa_n(i)]\sum_j [y_\nu(ij) + y_{\nu-1}(ji)]\exp[\kappa_n(i)] = 2\exp[2\kappa_n(i)]\sum_j y_n(ij)\exp[-2\kappa_n(i)] \tag{12}$$

We regard $\kappa_n(i)$ inside the summation as the input, and $\kappa_n(i)$ outside the summation as the output. We define the increment of $\kappa_n(i)$ as $\Delta\kappa_n(i)$:

$$\Delta\kappa_n(i) \equiv \kappa_n^{out}(i) - \kappa_n^{in}(i) \tag{13}$$

Then [12] can be rewritten as

$$\exp[-\Delta\kappa_n(i)]\sum_j [y_\nu(ij) + y_{\nu-1}(ji)] = 2\exp[2\Delta\kappa_n(i)]\sum_j y_n(ij) \tag{14}$$

For a binary system without vacancies, we can choose $\kappa_n(B) = 0$ because the sum of [5] for $i = A$ and B is always satisfied due to the normalization [1]. Then for $i = B$, [12] reduces to

$$\sum_j [y_\nu(Bj) + y_{\nu-1}(jB)] = 2\sum_j y_n(Bj) \tag{15}$$

When we form a ratio of [14] and [15], we obtain

$$\Delta\kappa_n(A) = \frac{1}{3}\ln\left\{\frac{\sum_j [y_\nu(Aj) + y_{\nu-1}(jA)]\sum_j y_n(Bj)}{\sum_j [y_\nu(Bj) + y_{\nu-1}(jB)]\sum_j y_n(Aj)}\right\} \tag{16}$$

This equation is to be solved iteratively for $\kappa_n(A)$ for all n. When the iteration has converged

$$\kappa_n^{out}(A) = \kappa_n^{in}(A) + \Delta\kappa_n(A) \qquad [17]$$

(iv) Minor Iteration for γ_n

We solve the other Lagrange multiplier $\gamma_n(i)$ together with $\kappa_n(i)$ in the minor iteration to satisfy [4]. Since the procedure is similar to that for solving $\kappa_n(i)$, we can skip some of the steps. The equation corresponding to [14] is

$$\exp(-\Delta\gamma_n(i))\sum_j y_{\nu-1}(ji) = \exp(\Delta\gamma_n(i))\sum_j y_\nu(ij) \qquad [18]$$

where we define

$$\Delta\gamma_n(i) \equiv \gamma_n^{out}(i) - \gamma_n^{in}(i) \qquad [19]$$

Since we define $\gamma_n(B) = 0$, [18] is solved as

$$\Delta\gamma_n(A) = \frac{1}{2}\ln\left[\frac{\sum_j y_{\nu-1}(jA)\sum_j y_\nu(Bj)}{\sum_j y_\nu(Aj)\sum_j y_{\nu-1}(jB)}\right] \qquad [20]$$

The iterative relations [16] and [20] are handled simultaneously.

(v) Major Iteration

Using $\kappa_n^{out}(1)$ and $\gamma_n^{out}(1)$, we can determine the output of $y_\nu(ij)$ and $y_n(ij)$ from [9]. First we set aside λ's and determine

$$y_\nu^0(ij) = y_\nu(ij)\exp(-\beta\lambda_\nu) \text{ and } y_n^0(ij) = y_n(ij)\exp(-\beta\lambda_n) \qquad [21]$$

from which and the normalization condition (1), we obtain

$$\exp(-\beta\lambda_\nu) = \sum_{ij} y_\nu^0(ij) \text{ and } \exp(-\beta\lambda_n) = \sum_{ij} y_n^0(ij) \qquad [22a]$$

Then we arrive at

$$y_\nu(ij) = y_\nu^0(ij)\exp(\beta\lambda_\nu)$$

$$y_n(ij) = y_n^0(ij)\exp(\beta\lambda_n) \qquad [22b]$$

The next input values $x_n(i)$ of the major iteration are calculated from these y's as

$$x_n(i) = \frac{1}{4}\sum_j [y_v(ij) + y_{v-1}(ji) + 2y_n(ij)] \qquad [23]$$

It was proved that the major iteration always converges [5]. The minor iteration converges very fast in one step except the initial stages for each major iteration.

(vi) Layer-thickness Constraint

Since the layer-structure is metastable, although we start with an initial structure of desired layer-thickness and symmetry, fluctuation can lead, for example, to widening of the hill region and the accompanying narrowing of the valley, to end up with the flat elongated hill composition, since such change can occur keeping the $\mu = 0$ intact. In order to prevent such change, we impose the condition that the width of the hill region is always kept fixed as the iteration proceeds. This condition is written in the following form, in which we write $m \equiv n_1$ to avoid a subscript on a subscript,

$$x_{m+n}(1) = 1 - x_{m-n+1} \qquad \text{for} \qquad n \le 1 \le m = n_1 \qquad [24]$$

PHASE SEPARATION DIAGRAM FOR A BULK FCC SYSTEM

For a homogeneous system, the phase separation diagram is calculated using the pair approximation for FCC by defining an auxiliary variable, θ, as

$$x_1 = \frac{\exp(6\theta)}{2\cosh(6\theta)}, \qquad \frac{x_1}{x_2} = \exp(12\theta)$$

and the temperature is

$$\exp(2\beta\varepsilon) = \frac{\sinh(6\theta)}{\sinh(5\theta)} \qquad [25]$$

where

$$4\varepsilon = 2\varepsilon(AB) - [\varepsilon(AA) + \varepsilon(BB)] \qquad [26]$$

Our choice of the sign is that $\varepsilon > 0$ in the present phase-separating system. We use the dimensionless reduced temperature as defined by

$$\tau \equiv \frac{kT}{\varepsilon} \qquad [27]$$

The critical point is given by

$$\tau_c = \frac{kT_c}{\varepsilon} = \frac{2}{\ln(6/5)} = 10.969630$$

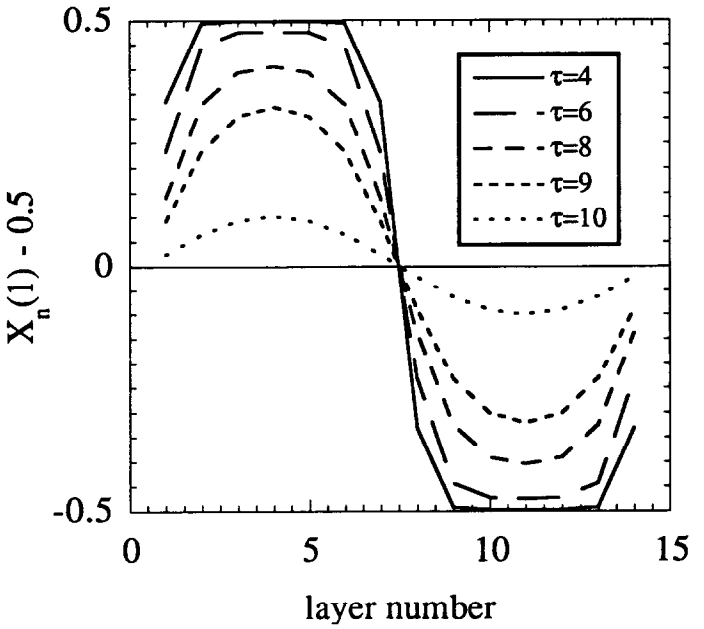

Figure 2. Composition profiles as a function of reduced temperature for the layer-structure with layer-thickness M = 7. Curves are for the reduced temperature $\tau = k_B T/\varepsilon = 4, 6, 8, 9$ and 10, from the outermost curve to the innermost.

THE PHASE DIAGRAMS FOR PERIODIC LAYER-STRUCTURES

The layer-structure is not a true equilibrium structure. Any perturbation should lead to coarsening. Therefore, it should be kept in mind that the equilibrium compositions obtained in this paper are under the constraint that the system is a periodic layer-structure. In this paper, we chose the simplest case that can be treated straightforwardly, namely the symmetric layer-structure, i.e., the α and β phases have the same thickness and $C_\alpha = 1 - C_\beta$.

An example of composition profiles, $x_n(1)$, at different temperatures is shown in Figure 2 for a layer-structure with layer-thickness M = 7. These curves are for reduced temperatures, τ = 4, 6, 8, 9 and 10, respectively as labeled in the figure. The hill and valley parts are chosen symmetric, so that every curve goes through $x_n(1) = 0.5$ at the middle point between a hill and a valley. The "layer-thickness", M, is defined as the number of lattice planes between the two neighboring $x_n(1) = 0.5$ positions.

In order to determine the dependence of the thermodynamic stability of layer-structure on layer-thickness, the composition profiles, $x_n(1)$, for different layer-thickness, but at the same temperature, $\tau = 8.0$, are shown in Figure 3. There are several interesting observations worthy to be pointed out. First of all, the composition profile across a junction does not change significantly for the layer-thickness larger than 8, which indicates that the thermodynamic properties of the

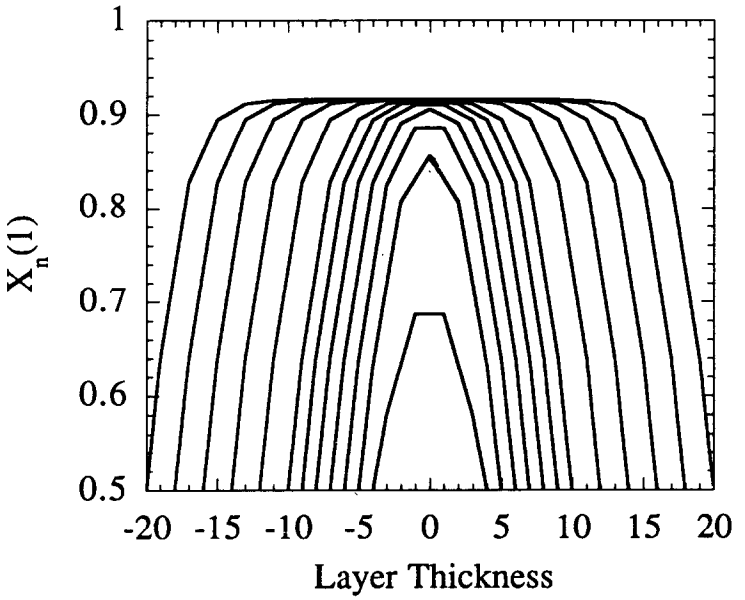

Figure 3. Comparison of the layer-structure $x_n(1)$ at $\tau = 8.0$ for different layer-thickness M. The right-hand side intersection of each curve with the 0.5 axis is equal to the M value for the curve.

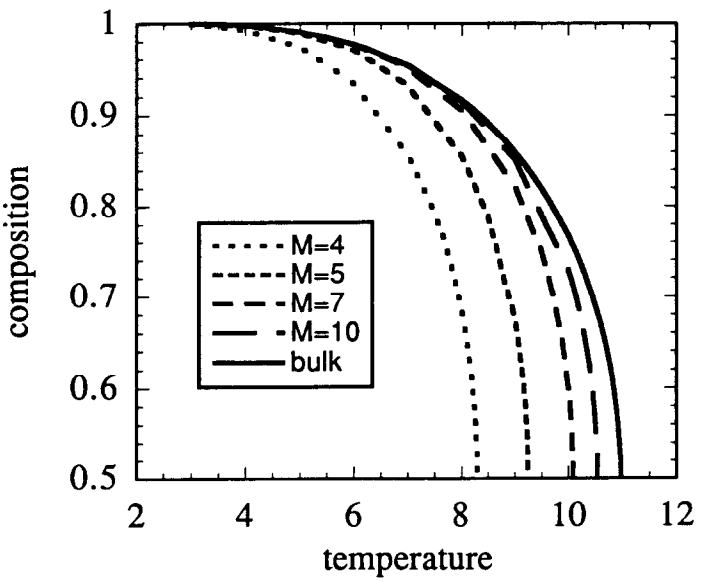

Figure 4. The maximum value of $x_n(1)$ at n = 0 for the M = 4, 5, 7 and 10 structures plotted against τ. The intersections with the 0.5 axis, i.e., the "critical" temperature τ_c, are 8.299, 9.292, 10.088 and 10.537 for M = 4, 5, 7 and 10, respectively. The phase separation curve for the bulk fcc with τ_c equal to 10.970 is also plotted for comparison.

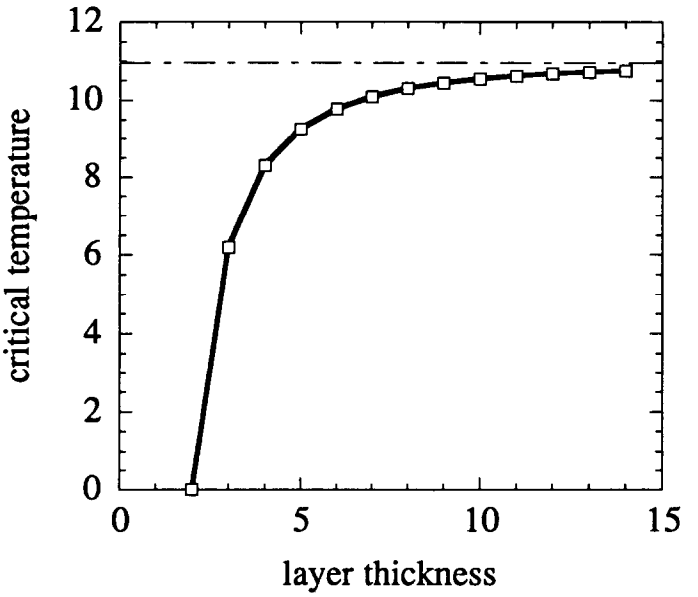

Figure 5. Plot of the critical temperature τ_c against the layer-thickness M. The horizontal line at the top is τ_c (M $\rightarrow \infty$) = 10.970 for the bulk system.

individual layers, more or less, behave the same as the corresponding bulk. Second, as the layer-thickness decreases to less than 8, the composition profile across the interface changes considerably. Moreover, the highest and lowest compositions deviate significantly from the corresponding bulk values as the layer thickness is reduced to less than 6. Finally, it is shown that for this temperature, M = 4 is the smallest stable layer-structure even though under the constraint the periodicity is maintained at all times.

From Figures 2 and 3, it is evident that the largest value of $x_n(1)$ for each τ and M curve appears at the position $n = 0$. We may interpret the highest and lowest values of the composition as the mutual solubilities for a particular temperature and layer-thickness. The dependence of this solubility as a function of temperature is plotted in Figure 4 for the layer-structure with M = 4, 5, 7 and 10. We can interpret these curves as the "phase diagrams" of the layered structures for these thicknesses. Since $x_{n=0}(1) = 0.5$ means that the system does not have the layer-structure any more, the temperature at $x_{n=0}(1) = 0.5$ in Figure 4 can be interpreted as the critical temperature, τ_c, for each M. For comparison, the phase separation curve for the bulk fcc alloy is also plotted in Figure 4. As is expected, the curve shifts towards the higher temperature side as M increases, and the bulk curve is higher than any finite M curve.

Figure 5 shows how τ_c varies with the layer-thickness, M. The homogeneous case is the limit $\tau_c(M = \infty) = 10.970$ as shown by the horizontal line. It is shown that the critical temperature decreases gradually as the layer-thickness decreases for M < 8, but it decreases sharply for M < 6. For M = 2, there is no stable layer structure.

The important implication of the results shown from Figures 2 - 5 is that the thermodynamic stability of periodic layer-structures varies significantly as the layer-thickness is reduced down to

a few nanometers. Our computer calculation predicted that the critical layer-thickness below which the bulk phase diagram is significantly modified is about 6 - 8 lattice spacings. For a typical FCC system with a typical lattice parameter 4 Å, this critical layer-thickness is about 12 - 16 Å (it is reminded that the lattice spacing for the (100) planes is half of the lattice parameter in the FCC lattice) or the critical periodicity of 24 - 32 Å. It is emphasized again that the miscibility gap or phase diagrams for different layer-thickness were obtained under the constraint that the system is completely periodic and symmetric. In practical systems, such periodic structures are subject to instability, the coarsening resulting in the increase in average layer-thickness. It is also to be remembered that the numerical estimate is based on the pair approximation of CVM.

CONCLUSIONS

The thermodynamic stability of periodic layer-structures of a binary phase-separating alloy (FCC) was examined using the pair approximation of CVM of equilibrium statistical thermodynamics. Deriving and solving the basic equations using the standard techniques of CVM under the constraint of a symmetric layer shape, it is shown that thermodynamic stability of periodic structures decreases sharply as the layer-thickness is reduced to less than a few nanometers. A system with a bulk miscibility gap may totally disappear when the layer-thickness decreases down to one to two lattice spacing in a periodic layer-structures.

ACKNOWLEDGEMENTS

We are grateful for the financial support from NSF under the grant number DMR-9311898 (LQC) and from ARPA under the NIST program on Modeling of Microstructure Evolution in Advanced Alloys (RK).

REFERENCES

1. R.E. Newnham, K.R. Udayakumar, and S. Trolier-Mckinstry, in *Chemical Processing of Advanced Materials*, eds. I.L. Hench and J.K. West, John Wiley and Sons, Inc., p. 379-393 (1992).
2. Ph. Buffat and J.P. Borel, Phys. Rev. A 13, 2287 (1976).
3. K. Ishikawa, K. Yoshikawa, and N. Okada, Phys. Rev. B 37, 5855 (1988).
4. R. Kikuchi, Phys. Rev. 81, 988 (1951).
5. R. Kikuchi, J. Chem. Phys. 60, 1071 (1974).